Antarct. Meteorite Res., **17**, 209–230, 2004

Petrology and reflectance spectroscopy of lunar meteorite Yamato 981031: Implications for the source region of the meteorite and remote-sensing spectroscopy

Takamitsu Sugihara[1*†], Makiko Ohtake[1], Atsuko Owada[2], Teruaki Ishii[3], Mayumi Otsuki[3] and Hiroshi Takeda[4]

[1]*Lunar Mission Research Center, Office of Satellite Technology, Research and Applications, National Space Development Agency of Japan, 2–1–1, Sengen, Tsukuba 305-0084*
[*]*Present address: Center for Deep Earth Exploration, Japan Agency for Marine-Science and Technology, 2–15, Natsushima-cho, Yokosuka 237-0061*
[2]*Advanced Engineering Service Co., 2–1–1, Sengen, Tsukuba 305-0084*
[3]*Ocean Research Institute, University of Tokyo, 1–15–1, Minamidai, Nakano-ku, Tokyo 164-0014*
[4]*Research Institute, Chiba Institute of Technology, 2–17–1, Tsudanuma, Narashino 275-0016*
[†]*Corresponding author. E-mail: sugiharat@jamstec.go.jp*

(Received September 20, 2002; Accepted June 8, 2004)

Abstract: Combined mineralogy and reflectance spectroscopy of lunar meteorite Yamato (Y) 981031 were investigated to determine its possible source region. Mineralogical observations indicate that Y981031 is a mixture of mafic mare and feldspathic highland components. Y981031 has abundant mineral fragments and lithic clasts in a comminuted matrix. Although the most of the lithic clasts are pyroxene-dominant basaltic clasts, some plagioclase-rich lithic fragments are also present. High- and low-Ca pyroxene grains with wide compositional variations are included in the breccia. Since high-Ca pyroxene ($Wo_{43}En_{40}Fs_{17}$ to $Wo_{29}En_{23}Fs_{48}$) and a part of Fe-rich low-Ca pyroxene are found in pyroxene-dominant basaltic clasts, they were derived from mare materials. In contrast, abundant Mg-rich low-Ca pyroxene (approximately $Wo_{10}En_{63}Fs_{27}$) is of highland origin because their chemical compositions resemble highland low-Ca pyroxene. Fusion crust glass compositions (TiO_2 = 0.50–0.77 wt% and FeO = 11.7–15.4 wt%) suggest that source mafic components of Y981031 have very low-Ti (VLT) affinity. In comparison with global remote-sensing data, the above TiO_2 and FeO concentrations resemble those of the VLT affinity in Mare Frigoris and adjacent maria. Thus, we propose that Y981031 was launched from this area. Modified gaussian model analysis of reflectance spectrum shows absorption features of high-Ca pyroxene (mare-origin) and Mg-rich low-Ca pyroxene (highland-origin), and enables us to observe separately mineralogical characteristics of each end member of Y981031 as the soil mixture.

key words: lunar meteorite, remote-sensing, reflectance spectroscopy, modified gaussian model, SELENE

1. Introduction

Approximately 25 lunar meteorites provide us with additional lunar materials that have not been sampled by the Apollo missions (*e.g.*, Arai *et al.*, 1996). Mineralogical

and petrological studies of these meteorites have considerably advanced our understanding of lunar materials (*e.g*., Arai *et al*., 1996; Fagan *et al*., 2002; Jolliff *et al*., 1998). However, it has been difficult to use such data to deduce ejection sites on the Moon, and to promote discussions of the origin of the meteorites for our better understanding of lunar material evolution.

Recently, global remote-sensing data such as Clementine VIS to NIR multiband images (415, 750, 900, 950, and 1000 nm in wavelength; Nozetto *et al*., 1994) have been employed as a powerful tool to understand the global distribution of surface materials on the Moon (*e.g*., Lucey *et al*., 1998, 2000; Giguere *et al*., 2000; Jolliff *et al*., 2000). The Clementine data enable us to obtain some elemental distribution maps of FeO and TiO_2 by employing some band calculation using the calibrated reflectance (*e.g*., Lucey *et al*., 2000). Thus, we can deduce some mineralogical and geochemical features of the entire Moon from the Clementine images. The Lunar Prospector gamma-ray spectrometer gave us radioactive elemental distribution maps of Th, U, K, Fe and some other elements (*e.g*., Lawrence *et al*., 2000). Therefore, remote-sensing data may be also a powerful tool to determine the ejection site of a lunar meteorite if they are combined with mineralogical and petrological data of the meteorite. Fagan *et al*. (2002) speculated on candidates for the source region of NWA032 by comparing bulk chemical compositions of the meteorite and remote-sensing data such as Lunar Prospector Th map and Clementine FeO map. Thus, we may be able to roughly determine the source region if we compare petrological characteristics of lunar meteorites with the remote-sensing data, especially with remote-sensing geochemical maps. However, the lunar surface soils are often mixtures of various kinds of rocks with different geochemical and mineralogical characteristics. Even if the chemical compositions of the soils are similar to those of a lunar meteorite, mineralogical characteristics of the soils may differ from those of the meteorite. Thus, detailed comparisons of the meteorite and remote-sensing data by only chemical compositions may not be possible to uniquely determine the ejection site of the meteorite.

Laboratory reflectance spectra measurements of lunar meteorites enable us to compare mineralogical characteristics of the meteorites with those of the lunar surface materials if we possess hyper spectral remote-sensing data with high spatial resolution acquired by lunar explorers. Some deconvoltion procedures for reflectance spectra can deduce separately spectroscopic characteristics of some individual constituents in a material mixture (*e.g*., Sunshine and Pieters, 1993). This approach can provide us with mineralogical and petrological characteristics of the surface soils in large areas in addition to geochemical data even if the soils are mixtures of brecciated rocks or soils with different characteristics. The meteorites can also provide "ground truth" data for the observed region in addition to the Apollo sample collections. However, similar studies have rarely been carried out because hyper spectral remote-sensing data for the entire moon is not available. Pieters *et al*. (1983) measured laboratory reflectance spectra of ALH81005, and they roughly estimated plausible source regions of the meteorite by combining reflectance spectra deduced from ground-based telescopic observations of the lunar surface and Apollo gamma-ray spectrometer data. Because their work utilized the ground-based spectral data with insufficient spatial resolution (10–20 km in length on the moon; McCord *et al*., 1981), they could not compare

laboratory reflectance data with the ground-based spectral data in detail.

Yamato (Y) 981031 is a lunar meteorite that has been proposed to be of mare-origin (Arai *et al*., 2002a). Preliminary studies on mineralogy, trace element geochemistry, and noble gas isotope geochemistry of Y981031 have been reported (Karouji *et al*., 2002; Nagao and Okazaki, 2002; Lorenzetti and Eugster, 2002; Arai *et al*, 2002a, b). Nagao and Okazaki (2002) and Lorenzetti and Eugster (2002) demonstrated that Y981031 and Y793274 are paired based on their similar exposure ages. Arai *et al*. (2002a, b) reported petrographical characteristics of the meteorite. However, the source region of the meteorite has not been discussed.

We conducted combined petrological and reflectance spectroscopic investigations of the meteorite to gain a better understanding of the ejection site of the meteorite and to acquire potential information as ground truth data for our future lunar mission. In this paper, we propose plausible source materials and a source region of Y981031 by comparing petrological characteristics and the elemental distribution map derived from the Clementine multi band images (Lucey *et al*., 2000). Then, we will combine spectroscopic characteristics of Y981031 with its petrological information to derive the origin of the spectroscopic characteristics. Based on this discussion, we examine possibility of hyperspectral observation by a lunar orbiter to determine the characteristics of lunar materials and to detect the source regions of lunar meteorites.

2. Methods

One polished thin section (PTS), Y981031,53-6 (10 mm × 4 mm; Fig. 1) and one fragment of Y981031,68 (0.130 g) were supplied by the National Institute of Polar Research (NIPR). After microscopic observations of PTS, 53-6, we obtained elemental distribution maps of Si, Al, Mg, Fe, K, Na, Ti, P, Cr and Ni to supplement the microscope observations by a JEOL 8900 electron probe micro-analyzer (EPMA) at the Ocean Research Institute (ORI), University of Tokyo, operating at 15 kV accelerating voltage and 50 nA probe current. Chemical compositions of minerals in PTS, 53–6, were also analyzed with a JEOL 733 EPMA at ORI, operating at 15 kV accelerating voltage and 12 nA probe current.

We measured UV-VIS-NIR bi-directional reflectance spectra of Y981031 by a JASCO reflectance spectrometer at the National Space Development Agency of Japan (NASDA). Powder samples for the reflectance measurement were prepared from a fragment of Y981031,68 by crushing in an agate mortar. The 0.130 g of sample powder was for grains sieved less than 75 μm in size. The reflectance spectra of this powder were measured as described below.

The spectrometer incidence angle was 30° and the emission angle was 0°. This photometric geometry is the same as that of Clementine multiband images (Eliason *et al*., 1999). The "Spectralon" reference standard was measured repeatedly during the measurements of the meteorite powder. The "Spectralon" is a diffuse reflectance standard material for the reflectance spectroscopy similar to Halon and is assumed to have a Lambertian surface (Weidner and Hsia, 1981). In this study, we report the sample reflectance data relative to the spectrum of the "Spectralon". Lunar standard soil 62231 collected by the Apollo 16 mission was repeatedly measured by the same

spectrometer in our laboratory at NASDA. The soil sample provides ground truth data of the lunar surface, and reflectances of the Clementine images were calibrated using the laboratory bi-directional reflectance of the 62231 soil measured at the Keck/NASA REFLECTANCE EXPERIMENT LABORATORY (RELAB; Pieters, 1999). To compare our laboratory reflectance spectrum with the RELAB reflectance data and the Clementine five-band spectra, we derived a spectral correction factor using the 62231 data measured at our laboratory and RELAB as described below:

$$\text{Correction factor} = \frac{\text{Clementine calibration reflectance of 62231}}{\text{NASDA laboratory reflectance of 62231}}.$$

Using this correction factor, we can compare our reflectance spectrum of Y981031 with the Clementine data eliminating any differences of instruments and measurement conditions between the two laboratories.

We estimate TiO_2 and FeO concentrations of the lunar surface soils in some maria by band calculations of the Clementine images between 415 and 750 nm for TiO_2 and 750 and 950 nm for FeO (Lucey *et al*., 1998, 2000). More detailed formulations of compositional derivation, their precision and accuracy, and problems for use are discussed in detail in Lucey *et al*. (1998, 2000). Effect of the soil maturity is also discussed in detail by many previous studies (*e.g*., Pieters *et al*., 2002; Taylor *et al*., 1999).

3. Results

3.1. Petrography and mineralogy

Y981031 is a polymict regolith breccia and contains a number of lithic clasts and mineral fragments in a dark comminuted matrix (Fig 1a). The mineral fragments are 100 to 500 μm in size and are composed of major pyroxene, plagioclase, and olivine including minor Fe-Ti oxide and Ca-phosphates. The matrix is not welded and is devoid of any material suggestive of remelting such as glass veins or glassy matrix (Fig. 1a). We consider that the absence of evidence of melting indicates that Y981031 was not affected by intense thermal effects during formation, brecciation and launching.

Y981031 contains four types of lithic clasts. Most of the clasts are mare basalt fragments composed of pyroxene and plagioclase with rare olivine and opaque minerals, and the chemical compositions of minerals in the clasts are similar to those of the mineral fragments. However, other lithic fragments seem to be of highland origin (Fig. 1b). A few clasts exhibit a metamorphic texture such as lunar granulites (Lindstrom and Lindstrom, 1986). The clasts are composed of An-rich plagioclase ($>An_{92}$) and low-Ca pyroxene ($Ca_8Mg_{64}Fe_{29}$), and resemble the granulitic clasts in highland fragmental breccias 60019 and Y86032 (Takeda *et al*., 1988). Glassy-matrix breccias and poikilitic breccias are also found in Y981031 as some lithic clasts with predominantly plagioclase fragments, which are common in the highland breccias. Therefore, these three types of clasts are of highland-origin (total modal abundance of the highland clasts is less than 10 vol%).

Chemical compositions of the mineral fragments were measured for fragments exceeding 100 μm in size to determine major rock components in precursor soils of

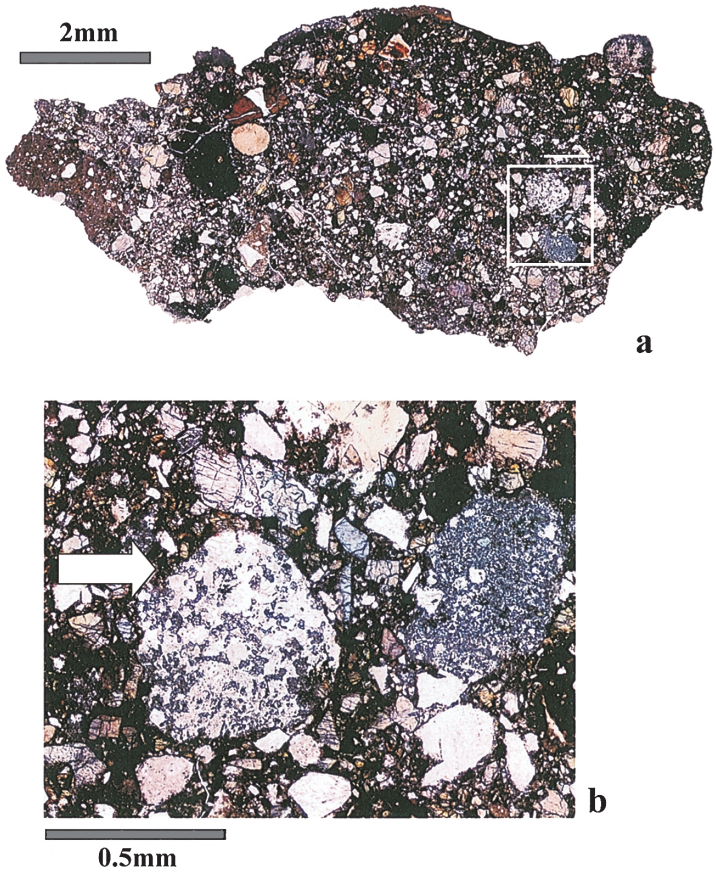

Fig. 1. Photomicrographs of Y981031 (open nicol). a: Overall view of Y981031. b: Granulitic lithic clast (white arrow) of highland origin. The area of photograph b is shown by a white square (right side of the square is upper side of b) in photograph a.

Y981031. Because most of the mineral fragments are over 100 μm in size (Fig. 1), our measurements would include general characteristics of the major components of the meteorite. Most of the mineral fragments are chemically homogeneous, and extensive chemical zoning within a fragment has not been found. Pyroxene chemical compositions are shown in Fig. 2.

Chemical compositions of pyroxene fragments in Y981031 (Fig. 2a) exhibit broad compositional variations. Compositions of high-Ca pyroxene ($Wo_{43}En_{40}Fs_{17}$ to $Wo_{29}En_{23}Fs_{48}$) are characterized by decreasing Ca component in the pyroxene quadrilateral with decreasing Mg# (Mg$\times$100/(Mg+Fe), atomic%) (Fig. 2a). Pyroxene in the mare basalt clasts is mainly high-Ca pyroxene, though a few pyroxene crystals with pigeonitic compositions have similar Mg#; this result is consistent with that of Arai *et al*. (2002a) (Fig. 2a). Thus, this high-Ca trend is composed of mare basalt components.

The compositional variation of low-Ca pyroxene is more ambiguous than that of

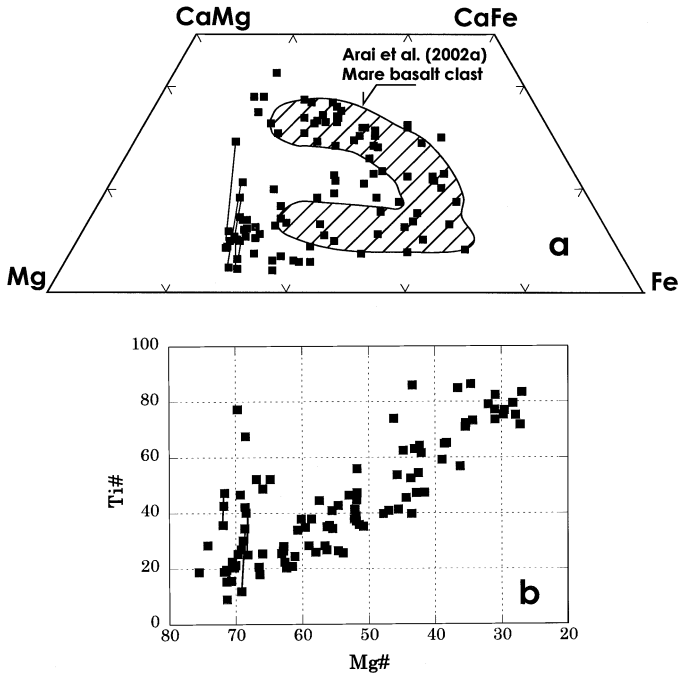

Fig. 2. Chemical compositions of pyroxene fragments in Y981031. a: Pyroxene compositions in pyroxene quadrilateral. b: Ti# (Ti×100/(Ti+Cr), atomic percent)–Mg# (Mg×100/(Mg+Fe), atomic percent) plot. The compositional range of the mare basalt clast in Y981031 (Arai et al., 2002) is also shown in the pyroxene quadrilateral (a). Tie lines between low-Ca and intermediate-Ca pyroxenes indicate compositional variation of exsolved pigeonite in one grain. Note these exsolved pigeonite crystals have a distinct chemical trend with broad Ti# and narrow Mg# variations in (b).

high-Ca pyroxene. In the most Mg-rich portion of the pyroxene compositional variation (Fig. 2a), compositions of individual electron microprobe analyses of these pyroxenes distribute relatively continuously between high and low-Ca pyroxene join ($Ca_{29}Mg_{54}Fe_{17}$ to $Ca_{18}Mg_{58}Fe_{23}$). Many pyroxene grains with pigeonitic bulk compositions are observed in this join (Fig. 2a). Pyroxene with these characteristics sometimes has exsolution lamellae, which can be optically observed with a petrographic microscope, and exhibits Ca compositional variation with similar Mg# in one grain. Therefore, these intermediate-Ca pyroxene compositions indicate several degrees of compositional averaging of high- and low-Ca exsolution lamellae of exsolved pigeonite by incomplete resolution of EPMA. These Mg-rich exsolved pigeonite grains are distinguishable from other pyroxene grains in a plot of Ti# (Ti×100/(Ti+Cr), atomic%) *vs*. Mg# plot (Fig. 2b). The Mg-rich pyroxene has broad Ti# variations, whereas Mg# variations are narrow. The low-Ca pyroxene in the granulitic clast mentioned above has nearly identical compositions to these Mg-rich exsolved pigeonites.

Some mineral fragments of relatively Fe-rich pigeonite are of mare material origin, because compositions of these pigeonite fragments overlap the compositional variation

of pyroxenes in the mare basalt clasts as shown above and by Arai *et al*. (2002a). There are also some orthopyroxene fragments ($Ca_4Mg_{60}Fe_{36}$–$Ca_5Mg_{67}Fe_{29}$) that are more iron-rich than the exsolved pigeonite mentioned above (Fig. 2a).

Chemical compositions of plagioclase fragments in Y981031 (Fig. 3) exhibit a wide range in anorthite (An) content ($An_{97.6}Ab_{2.4}Or_{0.02}$–$An_{50.5}Ab_{47.9}Or_{1.6}$), and relatively albite (Ab)-rich plagioclase crystals are also observed (up to An50; Fig. 3a). Such Ab-rich plagioclase crystals are rare in mare basalts and typical highland lithologies such as anorthosites and Mg-suite rocks, but have been typically found in KREEPy materials (BVSP, 1982; Papike *et al*., 1998). Although plagioclase grains in Y981031 have broad compositional variations in FeO and MgO contents compared to An content (Fig. 3b), we can divide them into two groups (high Fe-Mg trend and low Fe-Mg trend in Fig. 3b).

A large phosphate crystal (0.5 mm in size) is found in the thin section. The phosphate crystal has nearly pure Ca-apatite composition (Table 1).

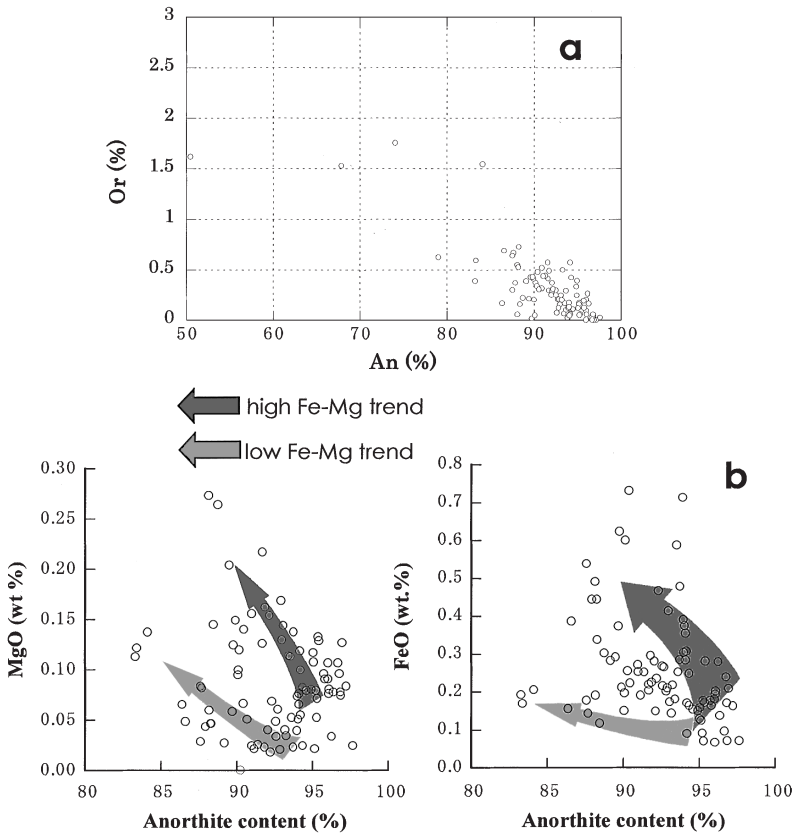

Fig. 3. Chemical compositions of plagioclase fragments in Y981031. a: Compositional relations between anorthite (An) and orthoclase (Or) compositions. b: Diagrams of MgO and FeO concentarations (wt%) versus An contents of plagioclase fragments in Y981031. Detection limit of MgO concentration determined by the EPMA is less than 0.02 wt%.

Table 1. Chemical compositions of apatite fragment.

	Core	Rim
SiO_2	0.27	0.26
TiO_2	0.02	0.05
Al_2O_3	0.57	0.04
FeO	0.71	0.43
MnO	0.02	0.03
MgO	0.02	0.00
CaO	51.26	52.51
P_2O_5	42.36	40.81
Total	95.22	94.17

Cl and F were not analyzed.

Table 2. Representative analyses of the glass fragments in Y981031.

	glass spherule								green glass	
	1	2	3	4	5	6	7	8	1	2
SiO_2	53.95	44.73	45.46	51.71	45.09	45.49	47.78	48.82	47.49	45.15
TiO_2	0.06	0.94	0.42	0.65	0.38	0.48	1.04	1.69	0.61	1.00
Al_2O_3	27.08	27.07	22.08	14.66	9.87	9.56	11.30	7.73	10.05	6.87
FeO	1.03	4.45	7.06	11.69	17.94	18.13	17.84	21.49	17.64	23.00
MnO	0.05	0.10	0.14	0.21	0.27	0.26	0.24	0.32	0.10	0.33
MgO	0.31	5.44	10.04	8.15	14.74	14.48	8.27	6.77	14.54	15.68
CaO	11.62	15.00	13.34	10.10	9.25	9.38	11.49	11.18	9.43	7.93
Na_2O	2.74	1.45	0.55	0.44	0.28	0.31	0.31	0.30	0.34	0.21
K_2O	1.83	0.06	0.03	0.21	0.01	0.00	0.07	0.05	0.06	0.00
Cr_2O_3	0.00	0.07	0.19	0.35	0.45	0.51	0.26	0.30	0.51	0.64
V_2O_3	0.00	0.04	0.03	0.03	0.03	0.06	0.00	0.11		
NiO	0.00	0.03	0.02	0.02	0.00	0.06	0.01	0.03		
P_2O_5	0.00	0.00	0.00	0.05	0.00	0.00	0.00	0.01		
Total	98.66	99.36	99.35	98.27	98.31	98.72	98.60	98.79	100.77	100.81
CaO/Al_2O_3	0.43	0.55	0.60	0.69	0.94	0.98	1.02	1.45	0.94	1.15

Chemical compositions of the green glass are after Shearer and Papike (1993).

Fragments of glass spherules are abundant in the thin section. They are clear to pale green in color and exhibit wide compositional ranges (Table 2). CaO/Al_2O_3 ratios of the glass spherules range from 0.43 to 1.45, and some spherules with relatively high CaO/Al_2O_3 ratios have a green glass-like chemical composition (Shearer and Papike, 1993). The green glass-like spherules were also reported by Arai *et al*. (2002a).

3.2. Fusion crust glass compositions

There is a dark yellow, glassy fusion crust on one side of the thin section. Minerals indicative of alteration, such as clay minerals, which are formed by terrestrial alteration after impact, are not apparent by microscopic observations of the fusion glass. Chemical compositions of the fusion glass are presented in Table 3 and Fig. 4, and are very

Table 3. Representative chemical analyses of the fusion crust glasses.

	fusion glass								bulk
No.	1	2	3	4	5	6	7	average (n=30)	
SiO_2	45.46	45.58	44.99	45.58	45.62	45.29	45.84	45.16	44.88
TiO_2	0.76	0.59	0.67	0.78	0.57	0.75	0.50	0.68	0.71
Al_2O_3	14.93	17.08	16.15	14.78	17.34	15.07	18.29	15.66	18.44
FeO	14.80	12.86	14.05	15.01	12.75	15.16	11.68	14.34	12.43
MnO	0.23	0.16	0.25	0.23	0.19	0.25	0.14	0.21	0.20
MgO	9.07	8.64	8.57	9.20	8.58	9.27	8.62	8.99	9.42
CaO	11.42	11.81	12.16	11.39	11.85	11.51	12.13	11.60	12.85
Na_2O	0.37	0.44	0.41	0.39	0.44	0.39	0.46	0.40	0.34
K_2O	0.08	0.07	0.09	0.08	0.12	0.05	0.07	0.07	0.04
Cr_2O_3	0.18	0.13	0.08	0.18	0.19	0.19	0.25	0.17	0.26
Total	97.30	97.35	97.42	97.62	97.64	97.92	97.97	97.28	99.57

The bulk chemical compositions of Y981031 are from Kojima *et al*. (2000).

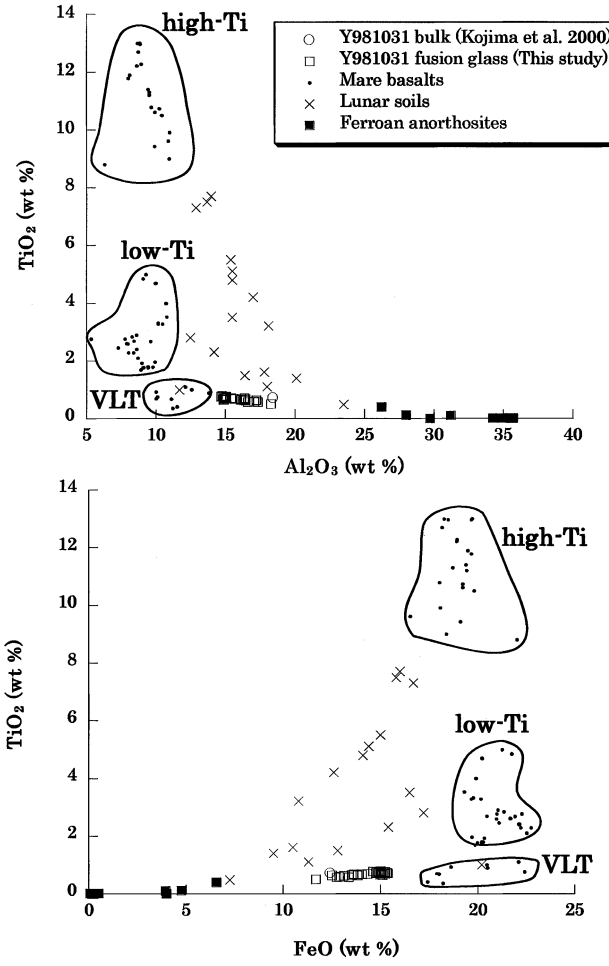

Fig. 4. Comparisons of the fusion glass chemical compositions of Y981031 with bulk chemical compositions of the mare basalts, surface soils, and highland materials plotted in the TiO_2-Al_2O_3 and TiO_2-FeO diagrams. The bulk chemical composition of Y981031 is after Kojima et al. (2000). The chemical compositions of fusion glass and bulk Y981031 compositions are similar and are plotted on the mixing line between the VLT basalts and highland materials (ferroan anorthosites, Taylor et al., 1993). The soil chemical compositions were from Papike and Simon (1982). The chemical compositions of the mare basalts and highland materials are from a review by Papike et al. (1998).

similar to the bulk chemical composition of Y981031 (Kojima *et al*., 2000), although compositional variations are also observed in the fusion glass (Sugihara *et al*., 2002). Compositional ranges of the fusion glass are TiO_2=0.50–0.77 wt%, Al_2O_3=14.7–18.3 wt%, and FeO=11.7–15.4 wt%. Compositions of individual electron microprobe analyses of this glass form a clear trend on each diagram (Fig. 4). These compositional variations are uniform and are not scattered, even if analytical errors of EPMA analysis are considered (up to a few percent relative error for analysis of each element). The bulk chemical compositions (TiO_2=0.71 wt%; Al_2O_3=18.44 wt%; FeO=12.43 wt%) determined by Kojima *et al*. (2000) that are plotted in the variation diagrams of the fusion glass (Fig. 4) are on the variation trend. Therefore, the chemical compositions of the fusion glass represent a well-mixed bulk rock chemical composition. The observed chemical variations may indicate different degrees of mixing between the

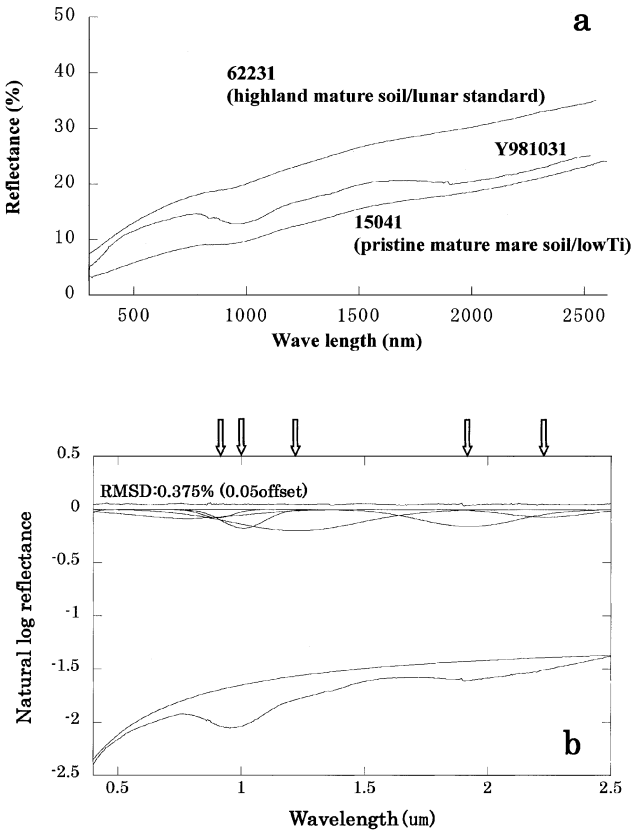

Fig. 5. Bi-directional reflectance spectrum and deconvolved results of Y981031. a: Reflectance spectrum of Y981031 as compared with the lunar soils 62231 and 15041. b: Deconvolved reflectance spectrum of Y981031. In b, RMS errors are presented in the uppermost part of the diagram with 0.05 offset. The reflectance spectrum of the 15041 mare soil is from Taylor et al. (2001); that of 62231 highland soil is from Pieters (1999). White arrows indicate positions of deconvolved absorption bands.

constituents in the meteorite.

3.3. Reflectance spectroscopy

In order to compare mineralogical and reflectance spectroscopic characteristics of Y981031, we measured the bi-directional reflectance spectrum of a powder created from Y981031,68 with particle sizes of less than 75 μm. The reflectance spectrum of the Y981031 finer fraction exhibits two broad absorption peaks at 1 and 2 μm (Fig. 5a).

The reflectance spectrum of Y981031 was deconvolved using a modified Gaussian model (MGM; Sunshine *et al*., 1990) and is shown in Fig. 5b. The reflectance spectrum gives us information about major mineral constituents with unique absorption features in the meteorite (*e.g*., Sunshine *et al*., 1990). Some silicate minerals containing Fe^{2+}, such as olivine and pyroxene, have characteristic absorption bands at approximately 1 and 2 μm (*e.g*., Burns, 1970). The reflectance spectra of Y981031 can be deconvolved into six absorption bands (0.78, 0.90, 1.01, 1.22, 1.92, 2.24 μm in wavelength; Fig. 5b); Fe^{2+} absorption bands at approximately 1 μm are divided into three absorption bands. They are observed at 0.90, 1.01, and 1.22 μm in wavelength. Two absorption bands are observed at 1.92 and 2.24 μm.

4. Discussions

4.1. Mixing of mafic mare and feldspathic highland components

Y981031 has both many of pyroxene-rich mafic clasts and a few clasts observed typically in highland breccias such as lunar granulites. Modal abundance of all of the highland clasts is less than 10%, and most of the clasts are mafic clasts. Therefore, we can propose that Y981031 is a mixture of mafic mare components and feldspathic highland components. Thus, we should also be able to observe mineral fragments that were derived from both components.

The high-Ca pyroxene trend (decreasing Mg# with decreasing Ca content as seen in the pyroxene quadrilateral in Fig. 2) is characteristic of mafic mare components (Fig. 2a). Although definition of low-Ca pyroxene compositional trends is difficult, relatively Fe-rich pigeonite crystals are of mare origin as discussed by Arai *et al*. (2002a). However, some orthopyroxene grains ($Ca_4Mg_{60}Fe_{36}$–$Ca_5Mg_{67}Fe_{29}$) might be derived from feldspathic highland material, because orthopyroxene is rare in the mare basalts (Papike *et al*., 1998; Takeda and Ridley, 1972).

As discussed below, the most Mg-rich exsolved pigeonite seems to be of highland-origin, though it is possible that this pyroxene is an early crystallization phase of the mafic mare components. The characteristics in the Ti#–Mg# plot of the Mg-rich pyroxene (Fig. 2b) resemble the chemical composition of one type of pyroxene in Y793274 (trend2; Arai *et al*., 1996). Arai *et al*. (1996) mentioned that pyroxene grains with a similar compositional trend might be derived from highland debris. Warren and Ulff-Møller (1999) found low-Ca pyroxene ($Wo_{3.5-9}$ En_{61-70}) with Ti#–Mg # characteristics similar to those of Mg-rich pigeonite of Y981031 in a highland-origin feldspathic lithic clast of EET96008. The chemical compositions of the low-Ca pyroxene are nearly identical to the Mg-rich exsolved pigeonite in Y981031. Korotev *et al*. (2003) showed that EET96008 and its pair EET87521 are launch paired with Y981031.

Therefore, the Mg-rich pigeonite in Y981031 may be derived from highland materials. This proposal is supported by the observation that low-Ca pyroxene observed in a granulitic clast of Y981031 has compositions identical to those of these Mg-rich exsolved pigeonites. Thus, although we cannot clearly define the compositional trend of low-Ca pyroxenes derived from mare materials, some of the pigeonite grains including orthopyroxenes, may be derived from the feldspathic highland materials.

Plagioclase grains with broad FeO and MgO compositional variations compared to An content (Fig. 3b) can be divided into two groups (high Fe-Mg trend and low Fe-Mg trend in Fig. 3b). Papike *et al*. (1998) mentioned that plagioclase in mare basalts has higher FeO and MgO concentrations than that in highland rocks with identical An content (*e.g*., Smith, 1974). The presence of two types of plagioclase might imply involvement of highland materials that have different petrological characteristics from the mare materials.

The chemical compositions of the glass spherules in Y981031 imply mixing of mafic mare and feldspathic highland materials. Table 1 indicates that the glass spherules in Y981031 have a wide compositional range, especially CaO/Al_2O_3 ratios, which range from 0.43 to 1.45. Arai *et al*. (2002a) noted that glass spherules in Y981031 are divided into two types, impact-origin and pyroclastic-origin, based on the Mg/Al ratio of the glass. A higher Mg/Al ratio indicates pyroclastic origin, and a lower one impact origin (Delano, 1986). However, Arai *et al*. (2002a) did not indicate the source region of the impact-origin spherules. The CaO/Al_2O_3 ratio is a useful parameter that can define the source region of the impact-origin glasses, though mare-origin and pyroclastic glasses cannot be distinguished well (Papike and Simon, 1982).

Papike and Simon (1982) indicated that the origin of glass spherules could be deduced from their chemical compositions. A higher (>0.75) CaO/Al_2O_3 ratio suggests that the glass is volcanic or an impact melt of the mare materials, whereas a lower ratio suggests an impact melt glass of highland materials. Plagioclase has the Al_2O_3-rich composition with less than 0.54 of the CaO/Al_2O_3 ratio, and the highland materials have high modal abundance of plagioclase. The glasses of highland origin may have lower CaO/Al_2O_3 ratios because of involvement of many plagioclase components. Thus, since Y981031 has many glass spherules with wide compositional ranges, we conclude that the glass spherules in Y981031 are mixtures of mare and highland glasses. Effective mixing of both types of glasses requires derivation of debris by impact ejecta or land slide from highland to the mare regions and disturbance of highland and mare soils by small impacts in the mare region. Therefore, precursor soils of Y981031 would occur in extensive mixing areas where impact glasses from the highland could be effectively derived. This result is consistent with descriptions of mineralogical observations of lithic clasts and mineral fragments, as mentioned above.

Thus, petrography and mineral chemistry indicate that Y981031 is a mixture of mafic mare and feldspathic highland components. The mixing would occur in extensive mixing areas near mare-highland contact (Warren, 1994).

4.2. Comparison of the reflectance spectrum with the mineralogical observations

The reflectance spectrum of Y981031 is compared with spectra of mature low-Ti mare soil 15041 and highland soil 62231 (Taylor *et al*., 2001; Pieters, 1999). An index

of maturity, Is (ferromagnetic resonance intensity)/FeO=93 for 15041 is reported by Taylor *et al*. (2001) and Is/FeO=91 for 62231 by Morris (1978). The reflectance spectrum of Y981031 apparently has clearer absorption bands than those of the mature soils, 62231 and 15041, indicating less maturity, though we did not measure Is/FeO of Y981031. However, a fragment of Y981031,68 was crushed in an agate mortar and then sieved. Thus, original mineral fragments in the meteorite must also be crushed into finer fragments, and this would expose and increase their fresh surfaces. Although we cannot estimate the effects of crushing, the reflectance spectrum of the meteorite may be fresher than that of a hypothetical compacted regolith of Y981031.

The reflectance spectrum of Y981031 can be deconvolved into six principle absorption bands as given previously (0.78, 0.90, 1.01, 1.22, 1.92, and 2.24μm in wavelength; Fig. 5b). Fe^{2+} absorption bands near 1μm are divided into three absorption bands (0.90, 1.01, and 1.22μm in wavelength), and two absorption bands close to 2μm are also observed (1.92 and 2.24μm). As mentioned above, Y981031 contains high-Ca pyroxene, low-Ca pyroxene, plagioclase, olivine and opaque minerals as mineral fragments, and pyroxene and plagioclase predominate as observed by petrographic microscope. The absorption features obtained using the MGM analysis should represent spectral characteristics of these minerals (Sunshine and Pieters, 1993, 1998; Pieters, 1996).

Figure 6 indicates the approximate contours of 1 and 2μm absorption wavelengths of pyroxene in the pyroxene quadrilateral (Cloutis and Gaffey, 1991) together with observed pyroxene chemical compositions. The deconvolved 0.90μm band corresponds to the absorption band of Mg-rich low-Ca pyroxene, although slight contrasts are

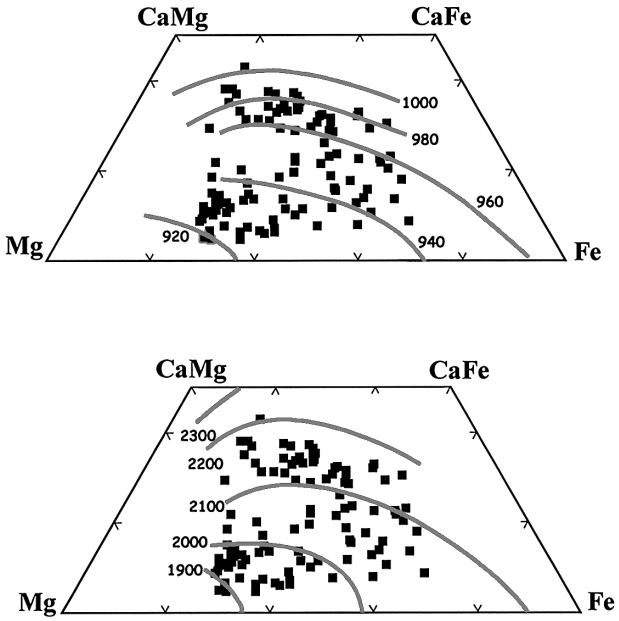

Fig. 6. Approximate contours of 1 and 2μm absorption bands of pyroxene plotted in Fig. 2a. The contours are from Cloutis and Gaffey (1991).

observed. The 1.01 μm band represents a high-Ca pyroxene chemical trend because the high-Ca pyroxene trend is almost parallel to the absorption contours. The absorption bands near 2 μm (1.92 and 2.24 μm) are consistent with absorption bands and chemical compositions of pyroxene with 1 μm peaks. The 1.92 μm band may represent Mg-rich low-Ca pyroxene, and the 2.24 μm band, a high-Ca pyroxene trend.

The 1.22 μm band can be attributed to the plagioclase and olivine mineral fragments and may represent mixed absorption features of both minerals (Sunshine and Pieters, 1998; Pieters, 1996). Although we cannot decide which mineral is more effective, plagioclase may display the predominant absorption characteristics because olivine is a minor constituent in Y981031.

The MGM can deconvolve the natural log of the reflectance spectrum into absorption bands, and each absorption band has an absorption depth proportional to the absorption energy (Sunshine *et al*., 1990). Two pyroxene absorption band pairs (0.90–1.92 μm pair and 1.01–2.24 μm pair) correspond to Mg-rich low-Ca pyroxene (possibly exsolved pigeonite in Fig. 2a) and to a high-Ca pyroxene compositional trend, suggesting that both phases predominate in Y981031. As mentioned in Section 4.1, we propose that Mg-rich low-Ca pyroxene (exsolved pigeonite) was derived from the highland materials, and high-Ca pyroxene, from mafic mare materials. Therefore, the reflectance spectrum of Y981031 also implies effective mare-highland mixing, and the MGM analyses successfully identify the mineralogical characteristics of both components.

4.3. Characteristics of source mafic mare components

Our fusion glass chemical compositions are consistent with well-mixed bulk rock chemical compositions, and the variations of the chemical compositions would indicate several degrees of mixing between the constituents of Y981031. Therefore, the fusion glass chemical compositions give us some information about source mafic mare components of Y981031, which have not been directly defined by the previous studies for Y981031.

In TiO_2-Al_2O_3 and TiO_2-FeO variation diagrams (Fig. 4), chemical compositions of some mare basalts, lunar mare regoliths and lunar highland rocks are compared to the fusion glass chemical compositions of Y981031 to deduce the source mafic mare components. On the TiO_2-Al_2O_3 diagram (Fig. 4), the mare regoliths are plotted on the mixing line between each Ti-type basalt and highland material (ferroan anorthosites; Taylor *et al*., 1993). A similar trend can be found on the TiO_2-FeO diagram (Fig. 4). These trends indicate that precursor mare regoliths of Y981031 were mixed with highland materials.

Our fusion glass chemical compositions of Y981031 are similar to those of very low-Ti (VLT) mare basalts, although the Al_2O_3 content is higher than those of the VLT basalts that were collected at the Apollo 17 and Luna 24 sites (Fig. 4). The variation of the fusion glass compositions is extrapolated to the VLT mare basalts region (Fig. 4), and the bulk rock chemical compositions (Kojima *et al*., 2000) are plotted on the variation line. Therefore, we propose that the source mafic components of Y981031 have the VLT mare basalts characteristics, at least for TiO_2 concentration, and are mixed with feldspathic highland components with higher Al_2O_3 and lower FeO concen-

trations. We cannot estimate the mixing ratio of the mafic VLT components and feldspathic highland components, because the chemical compositions (except for TiO_2 concentrations) of both end members are not constrained. However, the reflectance spectroscopy for Y981031 indicates effective mixing of the highland materials into the mare materials, therefore, the mixing ratio may not be so low.

Based on noble gas geochemical studies for Y981031, the meteorite is pared with Y793274 and launch paired with QUE94281 (YQ meteorites, Nagao and Okazaki, 2002; Lorenzetti and Eugster, 2002), since they have similar exposure ages. QUE94281 was also proposed to be launch paired with Y793274 by mineralogical study (Arai and Warren, 1999). Source basalts of Y793274 and QUE94281 (YQ meteorites) have been suggested to be VLT basalts (Takeda *et al*., 1992; Jolliff *et al*., 1998; Arai and Warren, 1999). Therefore, our result is consistent with these studies.

4.4. Relations with VLT basalts sampled by the previous missions

Pyroxene compositional trends of mafic VLT components in Y981031 (Fig. 2a) differ from those of Apollo 17 and Luna 24 VLT mare basalt fragments (BVSP, 1981). Although pyroxene chemical trends of slowly cooled Apollo 17 and Luna 24 VLT basalts are apparently similar to that of Y981031, high-Ca pyroxene compositional trends of the slowly cooled VLT basalts are more Ca-depleted and extend to more Fe-rich compositions than that of Y981031 (BVSP, 1981).

In addition to the mineralogical observations, Karouji *et al*. (2002) suggested that trace element compositions of Y981031 are different from those of the Apollo and Luna VLT basalts. They showed that the chondrite-normalized rare earth element (REE) pattern of Y981031 differs from those of Apollo 17 and Luna 24 VLT, and the VLT mare basalts sampled at Apollo 17 and Luna 24 sites have low trace element concentrations, including REE [chondrite-normalized La (La_n) = less than 10] and a light (L) REE-depleted pattern with a well-defined negative Eu anomaly (Papike *et al*, 1998), whereas Y981031 has relatively high REE concentrations (La_n = about 35), and an LREE-enriched pattern with a significant negative Eu anomaly (Karouji *et al*., 2002). This observation implies that source basalts or mixed highland materials or both have relatively high trace element concentrations. EET (Elephant Moraine) 87521 and 96008 have been proposed to be launch paired with Y981031 and the YQ meteorites (Korotev *et al*., 2003). Korotev *et al*. (2003) showed that the chemical compositions of clasts with approximately 17 wt% FeO in the EET meteorites represent those of the source of the mafic component of Y981031 (and paired YQ meteorites). Y981031 has lower FeO and higher Al_2O_3 abundances than those of the EET meteorites since Y981031 is a mixture of the mafic VLT affinity and highland materials as mentioned above. Karouji *et al*. (2002) also showed REE compositions of the EET meteorites, and the REE abundances of EET87521 and EET96008 (they have about 16 wt% FeO, which is similar to the estimated source composition of Y981031 by Korotev *et al*., 2003) are lower than those of Y981031 but higher than those of the VLT basalts collected by the Apollo and Luna missions, whereas the shape of their chondrite-normalized REE patterns is similar to that of Y981031 (Karouji *et al*., 2002). These characteristics indicate that the source VLT basalts of Y981031 are different from the Apollo and Luna VLT basalts, and mixed highland materials would have higher REE

(and other incompatible elements) abundances than those of Y981031 and the EET meteorites.

Therefore, the source region of Y981031 should also differ from those of the Apollo 17 and Luna 24 VLT basalts. Although we could not find a solid genetic relation of Y981031 to the previously refined VLT mare basalts, we refer to the VLT affinity as source basalts of Y981031 in the following discussion.

4.5. Source region of Y981031

We examined only one PTS in this study, but our results are in agreement with observations on other PTSs by other studies for some launch-paired meteorites of Y981031 (Arai and Warren, 1999; Jolliff *et al*., 1998; Warren and Ulff-Møller, 1999). Our descriptions of petrology and mineralogy are focused on aspects related the reflectance spectroscopy. We attempt to extraporate from mineralogy and petrology of one thin section to large area of the Moon. Because the proposed launch-parings are based on some common mineralogical features, we can justify that our PTS is representative of such pairs. We suggest that source lithologies of precursor regoliths of

Fig. 7. Clementine 750 nm mosaic showing distribution of the VLT basalts on the Moon. The VLT basalts are distributed only in the northeastern maria of the nearside Moon (Giguere et al., 2000). Y981031 might have been launched from these areas.

Y981031 had VLT characteristics in a broad sense (Fig. 4). As mentioned above, Y981031 has many launch-paired meteorites (YQ and EET meteorites), and Y981031 (and also Y793274) is a regolith breccia while other meteorites are fragmental breccias. A regolith breccia is expected to be located near surface. In addition, regolith breccias are products of ejection and mixing by repeated impacts of a large area around the ejection site. Even one PTS contains representative materials around the site. Therefore, we can compare geochemical and mineralogical characteristics of Y981031 with those of lunar global remote sensing data. Recent lunar exploration has given us global information of surface material distribution. Hence, we should be able to deduce a source region of Y981031 and the paired lunar meteorites by comparing petrological characteristics of Y981031 and remote-sensing data. According to the spectral analysis of the Clementine images, the VLT mafic basalts are located only in northeastern part of the nearside maria, mainly in Mare Frigoris, Lacus Somniorum, Lacus Mortis and northern Mare Crisium (Fig. 7; Giguere *et al*., 2000). We assume that Y981031 might have been launched from these broad areas where characteristics of the bedrock are similar. We admit that Y981301 might have been ejected from a very small-scale VLT region in the low- or high-Ti basalt region, or a small crypt mare region of VLT basalts (Head *et al*., 1993), because they cannot be identified by the remote-sensing data. However, we do not assume such very small regions for the source of Y981031.

We compared FeO and TiO_2 concentrations of the fusion glass of Y981031 and launch-paired Y793274 with those of regoliths in the northern maria region (Mare

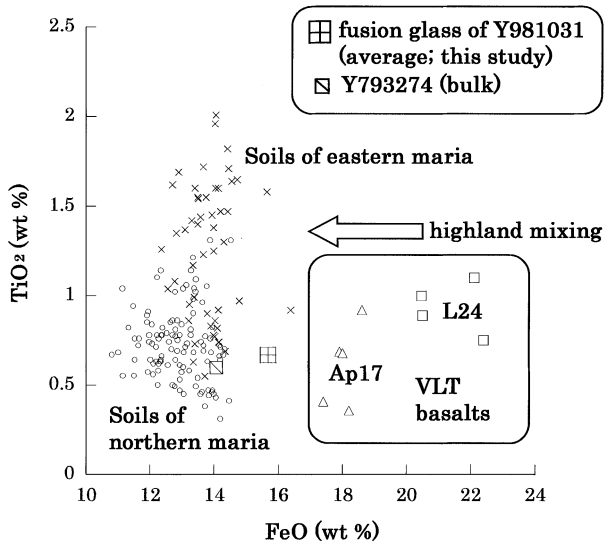

Fig. 8. Comparisons of TiO_2 and FeO compositions between averages of the fusion glass of Y981031 and surface soils in the VLT basalt regions. For comparison, Y793274, a meteorite proposed to be paired with Y981031 (Arai et al., 2002a; see text), is also plotted. The chemical compositions of Y793274 are from Arai et al. (1996). The TiO_2 and FeO concentrations of the surface soils were obtained by the Clementine images using Lucey et al. (2000) algorithms.

Frigoris, Lacus Somniorum, and Lacus Mortis) and eastern maria region (northern Mare Crisium) with the VLT characteristics (Fig. 8). We then derived the FeO and TiO_2 abundances (Fig. 8) of the soils of these maria from Clementine multispectral images using Lucey *et al*. (2000) algorithms. We acquired the spectral data of the mare basalt soils in each mare area from pixels of the Clementine images, and the data were uniformly acquired in this mare area including center of the mare to mare-highland contact. Acquired data thus reflect the effect of several degrees of mixing of the mare soils and the highland soils. The FeO and TiO_2 abundances of Y981031 (and Y793274) in Fig. 8 are more similar to those of the northern maria than to those of the eastern maria. We observed that the soils of the eastern maria are richer in TiO_2 abundances than Y981031 even if effects of highland material mixing are considered. Therefore, the northern maria (Mare Frigoris, Lacus Somniorum, and Lacus Mortis) are more plausible as the source region of Y981031 than the eastern maria (northern Mare Crisium).

Considering that Y981031 includes several types of highland materials (mineral fragments, some lithic clasts, and impact glasses), we believe that Y981031 is derived from the mare-highland contact as determined for other lunar meteorites by Warren (1994). Li and Mustard (2000) pointed out that lateral transport of highland material debris at the mare-highland contact is the most important phenomena for mixing mare materials with highland materials. Therefore, the mare-highland contact area in the northern maria region (Mare Frigoris, Lacus Somniorum, and Lacus Mortis) would be a plausible source region of Y981031. However, this discussion may not be appropriate considering that isolated crypt maria occur throughout the moon and may be possible source regions.

Our proposal is consistent with the following discussion. In Section 4.4, we pointed out the contribution of highland materials having higher incompatible element abundances than those of Y981031 based on results of Karouji *et al*. (2002). Jolliff *et al*. (2000) and Haskin *et al*. (2000) demonstrated that the crustal rocks around Mare Imbrium have high incompatible element (such as Th and REE) abundances using a Th abundance map derived from the Lunar Prospector gamma-ray spectrometer (*e.g*., Lawrence *et al*., 2000). Hence, contribution of trace element-enriched highland materials might be plausible in the northern maria region.

4.6. Possibility as ground truth of the lunar surface materials and implications for future research

As discussed in the last section, if we compare petrological characteristics of a lunar meteorite with the lunar remote-sensing geochemical map, we can roughly estimate a plausible source region of the meteorite. However, since most of mare soils on the lunar surface are affected by several degree of mixing with highland materials (Papike and Simon, 1982; Li and Mustard, 2000), we may not be able to determine petrological characteristics of subsurface bedrock and to estimate the source region of a lunar meteorite by only comparing geochemical data of the meteorite and remote-sensing data. Based on the result of the MGM analyses in this paper, if we can obtain global reflectance spectrum data with high spectral and spatial resolution and compare them with our laboratory data, we can separately understand mineralogical characteristics of

both mare and highland materials and accurately define the source region of the meteorite in more detail from remote-sensing data using the MGM analyses. Hence, the meteorite would provide us with ground truth data of the region. However, since Clementine spectral images have only 5 bands (Nozette *et al*., 1994), we cannot compare the laboratory reflectance data in detail. The Japanese SELENE lunar mission will be launched in 2005 to explore lunar global material distribution in more detail than the past lunar missions such as Clementine and Lunar Prospector. SELENE will carry the Spectral Profiler (SP), which will acquire global reflectance spectra (0.5 to 2.6μm in wavelength) with high spatial resolution (about 500 m; Matsunaga *et al*., 2000). We will try to precisely locate source areas of the lunar meteorites using SP data, and the lunar meteorites will provide us with ground truth data around the source area as combined with other geochemical remote-sensing instruments on SELENE, including Multi band Imager and/or X-ray spectrometer.

5. Conclusions

(1) Mineralogical and petrological data, especially the fusion glass chemical compositions plotted in TiO_2-Al_2O_3 and TiO_2-FeO diagrams, indicate that the source of mafic components in Y981031 have affinity to "VLT mafic basalts" mixed with highland materials.

(2) The TiO_2 and FeO concentrations of Y981031 deduced from fusion glass compositions resemble those of VLT basalt soils in the northern maria region on the Clementine TiO_2 distribution map (Mare Frigoris, Lacus Somniorum, and Lacus Mortis). Thus, we propose that Y981031 might have been derived from this region.

(3) Deconvolution of the Y981031 reflectance spectrum revealed the presence of two types of pyroxene absorption band pairs, (0.90–1.92μm and 1.01–2.24μm), and these data are consistent with the chemical compositions of pyroxene fragments.

(4) Although we can roughly compare spectral and geochemical characteristics of the meteorites with those of lunar soils by processing multi band images such as acquired by Clementine, if we can obtain global reflectance spectrum data with high spectral and spatial resolution, we will be able to deduce materials with characteristics of several end members and to precisely define the source region of the meteorite from future remote-sensing data.

Acknowledgments

We thank the National Institute of Polar Research for providing us with the samples for this work. This work was supported in part by a grant from the Ocean Res. Inst., Univ. of Tokyo, and is conducted as a part of "Ground Research for SELENE Mission" promoted by the LISM group. Additional support came from NASDA grants 9–43 to one of the authors (TS). We are grateful to Drs. Naru Hirata, Hirohide Demura, Junichi Haruyama and other co-workers of the Lunar Mission Research Center of NASDA for many helps and encouragement. Helpful comments of Dr. P. Buchanan, Dr. R.L. Korotev and an anonymous reviewer improved the manuscript considerably. We are indebted to Prof. Hideyasu Kojima and Dr. Takahiro Hiroi for

useful discussions.

References

Arai, T. and Warren, P.H. (1999): Lunar meteorite Queen Alexandra Range 94281: Glass compositions and other evidence for launch paring with Yamato 793274. Meteorit. Planet. Sci., **34**, 209–234.

Arai, T., Takeda, H. and Warren, P.H. (1996): Four lunar mare meteorites: Crystallization trends of pyroxenes and spinels. Meteorit. Planet. Sci., **31**, 877–892.

Arai, T., Ishi, T. and Otsuki, M. (2002a): Mineralogical study of a new lunar meteorite Yamato 981031. Lunar and Planetary Science XXXIII. Houston, Lunar Planet. Inst., Abstract #2064 (CD-ROM).

Arai, T., Ishii, T. and Otsuki, M. (2002b): A new lunar meteorite Yamato 981031: A possible link between two lunar-meteorite source craters. Antarctic Meteorites XXVII. Tokyo, Natl Inst. Polar Res., 4–6.

Burns, P.M. (1970): Mineralogical Applications to Crystal Field Theory. NewYork, Cambridge University Press, 224 p.

BVSP (Basaltic Volcanism Study Project) (1981): Basaltic Volcanism on the Terrestrial Planets. NewYork, Pergamon, 1286 p.

Cloutis, E.A. and Gaffey, M.J. (1991): Pyroxene spectroscopy revisted: Spectral-compositional correlations and relationship to geothermometry. J. Geophys. Res. **96**, 22809–22826.

Delano J.W. (1986): Pristine lunar glasses: Criteria, data and implications. Proc. Lunar Planet. Sci., 16th, Pt. 2, D201–D213 (J. Geophys. Res., **91**, B4).

Eliason, E.M., McEwen, A.S., Robinson, M.S., Lee, E.M., Becker, T., Gaddis, L., Weller, L.A., Isbell, C.E., Shinaman, J.R., Duxbury, T. and Malaret, E. (1999): Digital processing for a global multispectral map of the moon from the Clementine UVVIS imaging instrument. Lunar and Planetary Science XXX. Houston, Lunar Planet. Inst., Abstract #1933 (CD-ROM).

Fagan, T.J., Taylor, G.J., Keil, K., Bunch, T.E., Wittke, J.H. *et al*. (2002): Northwest Africa 032: Product of lunar volcanism. Meteorit. Planet. Sci., **37**, 371–394.

Giguere, T.M., Taylor, G.J., Hawke, B.R. and Lucey, P.G. (2000): The titanium contents of lunar mare basalts. Meteorit. Planet. Sci., **35**, 193–200.

Haskin, L.A., Gillis, J.J., Korotev, R.L. and Jolliff, B.L. (2000): The materials of the lunar Procellarum KREEP Terrane: A synthesis of data from geomorphological mapping, remote sensing, and sample analyses. J. Geophys. Res., **105**, 20403–20415.

Head, J.W., Mustard, J., Antonenko, I. and Hawke, B.R. (1993): Modes of formation of lunar light plains and the detection of crypt maria deposits. Lunar and Planetary Science XXIV. Houston, Lunar Planet. Inst., 629–630.

Jolliff, B.L., Korotev, R.L. and Rockow, K.M. (1998): Geochemistry and petrology of lunar meteorite Queen Alexandra Range 94281, a mixed mare and highland regolith brecchia, with special emphasis on very-low-titanium mafic components. Meteorit. Planet. Sci., **33**, 581–601.

Jolliff, B.L., Gillis, J.J., Haskin, L.A., Korotev, R.L. and Wieczorek, M.A. (2000): Major lunar crustal terranes: Surface expressions and crust-mantle origins. J. Geophys. Res., **105**, 4197–4216.

Karouji, Y., Oura, Y. and Ebihara M. (2002): Chemical composition of lunar meteorites including Yamato 981031. Antarctic Meteorites XXVII. Tokyo, Natl Inst. Polar Res., 52–54.

Kojima, H., Kaiden, H. and Yada, T. (2000): Meteorite search by JARE-39 in 1998–99 seasons. Antarct. Meteorite Res., **13**, 1–8.

Korotev, R.L., Jolliff B.L., Zeigler R.A. and Haskin L.A. (2003): Compositional evidence for launch pairing of the YQ and Elephant Moraine lunar meteorites. Lunar and Planetary Science XXXIV. Houston, Lunar Planet. Inst., Abstract #1357 (CD-ROM).

Lawrence, D.J., Feldman, W.C., Barraclough, B.L., Binder, A.B, Elphic, R.C., Maurice, S., Miller, M.C. and Prettyman, T.H. (2000): Thorium abundances on the lunar surfaces. J. Geophys. Res., **105**, 20307–20331.

Li, L. and Mustard, J.F. (2000): Compositional gradients across mare-highland contacts: Importance and geological implication of lateral transport. J. Geophys. Res., **105**, 20431–20450.

Lindstrom, M.M. and Lindstrom, D.J. (1986): Lunar granulites and their precursor anorthositic norites of

the early lunar crust. Proc. Lunar Planet. Sci. Conf., 16th, Pt. 2, D263–D276 (J. Geophys. Res., **91**, B4).

Lorenzetti, S. and Eugster, O. (2002): Noble gas characteristics of lunar meteorite Yamato-981031 paired with basaltic-anorthositic breccia Yamato-793274. Antarctic Meteorites XXVII. Tokyo, Natl Inst. Polar Res., 75–76.

Lucey, P.G., Blewett, D.T. and Hawke, B.R. (1998): Mapping the FeO and TiO_2 content of the lunar surface with multispectral imagery. J. Geophys. Res., **103**, 3679–3699.

Lucey, P.G., Blewett, D.T. and Jolliff, B.L. (2000): Lunar iron and titanium abundance algorithms based on final processing of Clementine ultraviolet-visible images. J. Geophys. Res., **105**, 20297–20305.

Matsunaga, T., Ohtake, M., Hirahara, Y. and Haruyama, J. (2000): Development of a visible and near infrared spectrometer for Selenogical and Engineering Explorer (SELENE). Proc. SPIE., **4151**, 32–39.

McCord, T.B., Clark, R.N., Hawke, B.R., McFadden, L.A. and Owensby, P.D. (1981): Moon: Near-infrared spectral reflectance, A first good look. J. Geophys. Res., **86**, 10883–10892.

Morris, R.V. (1978): The surface exposure (maturity) of lunar soils: Some concepts and Is/FeO compilation. Proc. Lunar Planet. Sci. Conf., **9th**, 2287–2298.

Nagao, K. and Okazaki, R. (2002): Noble gases of Yamato 981031 lunar meteorite. Antarctic Meteorites XXVII. Tokyo, Natl Inst. Polar Res., 107–109.

Nozette, S., Rustan, P., Pleasance, L.P., Horan, D.M., Regeon, P. *et al*. (1994): The Clementine mission to the Moon: Scientific overview. Science, **266**, 1835–1839.

Papike, J.J. and Simon, S.B. (1982): The lunar regolith: Chemistry, mineralogy, and petrology. Rev. Geophys. Spacephys., **20**, 761–826.

Papike, J.J., Ryder, G. and Shearer, C.K. (1998): Lunar samples. Planetary Materials, ed. by J.J. Papike. Washington, D.C., Mineral. Soc. Am., 5-1–5-234 (Reviews in Mineralogy, Vol. 36).

Pieters, C.M. (1996): Plagioclase and maskelynite diagnostic features. Lunar and Planetary Science XXVII. Houston, Lunar Planet. Inst., 1031–1032.

Pieters, C.M. (1999): The moon as a spectral calibration standard enabled by lunar samples: The Clementine example. New Views of the Moon II: Understanding the Moon through the Integration of Diverse Datasets. Flagstaff, #8025.

Pieters, C.M., Hawke, B.R., Gaffey, M. and McFadden, L.A. (1983): Possible lunar source areas of meteorite ALHA81005: Geochemical remote sensing information. Geophys. Res. Lett., **10**, 813–816.

Pieters, C., Taylor, L.A. and the LSCC (2002): The perplexing role of TiO_2 in the evolution of lunar soils. Lunar and Planetary Science XXXIII. Houston, Lunar Planet. Inst., Abstract #1866 (CD-ROM).

Shearer, C.K. and Papike, J.J. (1993): Basaltic magmatism on the Moon: A perspective from volcanic picritic glass beads. Geochim. Cosmochim. Acta, **57**, 4785–4812.

Smith, J.V. (1974): Lunar mineralogy: A heavenly detective story. Part I. Am. Mineral., **59**, 231–243.

Sugihara T., Ohtake, M., Takeda H., Owada A., Ishii T. and Otsuki M. (2002): Petrology and reflectance spectroscopy of a lunar meteorite Y981031. Antarctic Meteorites XXVII. Tokyo, Natl Inst. Polar Res., 154–156.

Sunshine, J.M. and Pieters, C.M. (1993): Estimating modal abundances from the spectra of natural and laboratory mixtures using Modified Gaussian Model. J. Geophys. Res., **98**, 9075–9087.

Sunshine, J.M. and Pieters, C.M. (1998): Determining the composition of olivine from reflectance spectroscopy. J. Geophys. Res., **103**, 13675–13688.

Sunshine, J.M., Pieters, C.M. and Pratt, S.F. (1990): Deconvolution of mineral absorption bands: An improved approach. J. Geophys. Res., **95**, 6955–6966.

Takeda, H. and Ridley, W.I. (1972): Crystallography and chemical trends of orthopyroxene-pigeonite from rock 14310 and coarse fine 12033. Geochim. Cosmochim. Acta, **1**, 423–430.

Takeda, H., Miyamoto, M., Mori, H. and Tagai, T. (1988): Mineralogical studies of clasts in lunar highland regolith breccia 60019 and in lunar meteorite Y82192. Proc. Lunar Planet. Sci., **18th**, 33–43.

Takeda, H., Mori, H., Saito, J. and Miyamoto, M. (1992): Mineralogical studies of lunar mare meteorites EET87521 and Y793274. Proc. Lunar Planet. Sci., **22**, 355–364.

Taylor, L.A., Pieters, C., Patchen, A., Morris, R.V., Keller, L.P., Wentworth, S. and Mckay, D.S. (1999): Apollo 17 soil characterization for reflectance spectroscopy. New Views of the Moon II: Understand-

ing the Moon through the Integration of Diverse Datasets. Flagstaff, #8041.
Taylor, L.A., Pieters, C.M., Keller, L.P., Morris, R.V. and Duke, M. (2001): Lunar mare soils: space weathering and the major effects of surface-correlated nanophase Fe. J. Geophys. Res., **106**, 27985–28000.
Taylor, S.R., Norman, M.D. and Esat, T.M. (1993): The Mg-site and the highland crust: An unsolved enigma. Lunar and Planetary Science XXIV. Houston, Lunar Planet. Inst., 1413–1414.
Warren, P.H. (1994): Lunar and Martian meteorite delivery services. Icarus, **111**, 338–363.
Warren, P.H. and Ulff-Møller (1999): Lunar meteorite EET96008: Paired with EET87521, but rich in diverse clasts. Lunar and Planetary Science XXX. Houston, Lunar Planet. Inst., Abstract #1450 (CD-ROM).
Weidner, V.R. and Hsia, J.J. (1981): Reflection properties of pressed polytetrafluoroethylene powder. J. Optic. Sci. Am., **71**, 856–861.